



Experimental study of wave overtopping of coastal protections for sea state combining swell and wind waves

**Antoine VILLEFER^{1,2}, Michel BENOIT^{1,2}, Damien VIOLEAU^{1,2},
Maria TELES¹, Christopher LUNEAU³**

1. EDF R&D, Laboratoire National d'Hydraulique et Environnement (LNHE), Chatou, France.
2. Laboratoire d'Hydraulique Saint-Venant (LHSV) (Ecole des Ponts, EDF R&D), Chatou, France.
3. OSU Institut Pythéas, Aix Marseille Univ, CNRS, IRD, Marseille, France.
*antoine.villefer@protonmail.com ; michel.benoit@edf.fr ; damien.violeau@edf.fr ;
maria.teles@edf.fr ; christopher.luneau@osupytheas.fr*

Abstract:

To protect coastal areas against the risk of wave submersion in storm conditions, coastal protections are required. Most often, these are designed in relation to a permissible wave overtopping rate. In the literature, numerous references, regularly updated, propose methods for estimating this overtopping rate (e.g. EurOtop 2018). However, the application of these methods to a bimodal sea state combining a swell, originating offshore, and wind waves, formed by a local wind, raises questions. Are the average characteristics of this complex sea state (i.e. a significant wave height and a wave period) sufficient to estimate the wave overtopping rate? To answer this question, a model of a coastal breakwater was built in the wave tank of the OSU Institut Pythéas in Marseilles (France). Considering a breakwater with a 3:2 (H:V) slope, two types of slope surface were tested: a smooth, impermeable one and a rock-armored one. The tests carried out showed that, for these choices of breakwater and for the sea states considered, existing empirical formulas tend to overestimate wave overtopping rates when the proportion of wind waves in the total energy of the sea state is high. This overestimation is more pronounced in the presence of a rock armor. It would appear that a rock-armored slope is more effective at damping wind-wave energy than swell energy.

Paper selected during the colloquium

"XVIIèmes Journées Nationales Génie Côtier Génie Civil", Chatou (France), 11-13 October 2022.

Received 21 September 2023, accepted 13 January 2024, available online 10 June 2024.

Short translated version not certified, published under the responsibility of the authors.

How to cite the original paper:

VILLEFER A., BENOIT M., VIOLEAU D., TELES M., LUNEAU C. (2024). *Étude expérimentale de submersion de protections côtières pour des états de mer combinant houle et clapot*. Revue Paralia, Vol. 14, pp s02.1–s02.12. DOI: <https://doi.org/10.5150/revue-paralia.2024.s02>

1. Introduction

Storms impacting coastal areas lead to the formation of extreme sea states, which can cause significant damage to seaside infrastructures and natural coastal relief. To protect against these hazards, coastal structures are often installed. In the scientific literature, numerous references propose recommendations for the design of these protections, such as TAW (2002), PULLEN *et al.* (2007) referred to as EurOtop (2007) and VAN DER MEER *et al.* (2018) referred to as EurOtop (2018). Based on the infrastructure's permissible wave overtopping rate and incident sea conditions, these references propose empirical formulas for determining the characteristics and dimensions of the protective structure.

During these extreme events, sea states are often composed of several wave systems, identifiable by their wavelengths or incoming directions. Commonly used empirical formulas (e.g. EurOtop 2018) propose an estimate of the mean wave overtopping rate based on a sea state described by three physical parameters: significant wave height, wave period and direction. The present study aims to verify the validity of using these parameters alone to describe the complexity of observed bimodal sea states in order to estimate wave overtopping rates. For this purpose, we have chosen to study the case of wave overtopping of coastal protections for a sea state composed of a swell, long waves coming from the open sea, and wind waves, short waves generated locally by the wind, both coming from the same direction normal to the structure. Both wave systems are thus differentiated by their wavelengths (and wave periods) and, to a lesser extent, by their significant wave heights.

A model of coastal breakwater with a 3:2 (H:V) slope was built and installed in the wind-wave tunnel of the OSU Institut Pythéas in Marseilles (France). The model was designed so as to be able to vary its freeboard height, i.e. the difference in height between the breakwater's crest elevation and the mean water level. Two types of slope surface were tested: a smooth, impermeable one and a rock-armored one. Using the mechanical wavemaker, wave overtopping rates were studied for a wide variety of bimodal sea states, each described by a wave height-wave period pair. Wave overtopping rates are recorded in different configurations and compared with estimations according to various empirical formulas.

In § 2 of this article, several empirical formulas for estimating the wave overtopping rate are presented. § 3 describes the physical model, while § 4 presents the results obtained and opens a discussion on ways of improving the empirical formulas described in § 2. A conclusion (§ 5) closes the present study by suggesting further experiments.

2. Estimation of wave overtopping rates

In the literature, numerous references propose methods for estimating the mean wave overtopping rate q (in m^2/s) as a function of the characteristics of the coastal protection

and the incident sea state. We limit ourselves here to the case of waves with normal incidence on the structure.

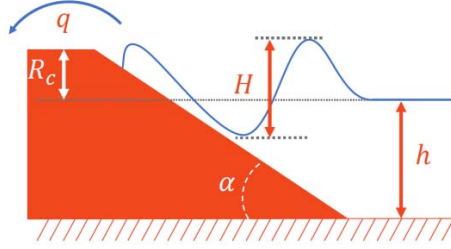


Figure 1. Definition sketch of the wave overtopping process. The orange breakwater illustrates the breakwater slope considered in our study. ($\cotan \alpha = 3/2$).

Although there are differences between these methods, they are all based on the following dimensional analysis:

$$q = f(g, H_s, L_m, R_c, \alpha) \quad (1)$$

where g is the acceleration due to gravity, H_s the significant wave height (i.e. H_{m_0} or $H_{1/3}$), L_m is the representative wavelength in deep water, R_c the crest freeboard and α the angle characterizing the breakwater slope ($\cotan \alpha = 3/2$ here).

The surf-similarity parameters (defined after Eq. (5) below) corresponding to sea states considered in this study are sufficiently high (> 3) to ensure that waves do not break either before the breakwater or on it. Following the recommendations of references such as EurOtop (2018), we therefore assumed that the water depth h is not explicitly considered in the calculation of the wave overtopping rate. It does, however, implicitly affect the significant wave height measured at the toe of the breakwater. This assumption, commonly adopted in similar studies, has no impact on the applicability of the results.

The dispersion relation for waves in deep water gives $L_m = gT_m^2/(2\pi)$ with T_m the corresponding period. As suggested in EurOtop (2018), this dispersion relation is used whatever the water depth h at the toe of the structure to define the representative wave steepness s_m . Since the only quantities involved are lengths and durations, the Vaschy-Buckingham theorem proves the existence of four dimensionless numbers to describe the problem:

$$\frac{q}{\sqrt{gH_s^3}} = F\left(\frac{R_c}{H_s}, \frac{H_s}{L_m}, \tan \alpha\right) \quad (2)$$

The following notations are used for dimensionless variables:

$$q^* = \frac{q}{\sqrt{gH_s^3}} \quad ; \quad R_c^* = \frac{R_c}{H_s} \quad ; \quad s_m = \frac{H_s}{L_m} \quad (3)$$

Existing methods for estimating wave overtopping rates can be divided into two families of empirical formulas based on the exponential function. OWEN (1980) proposed the following formula:

$$q^* \sqrt{\frac{s_m}{2\pi}} = a \exp \left(-b \frac{R_c^*}{\gamma_f} \sqrt{\frac{s_m}{2\pi}} \right) \quad (4)$$

with (a, b) a pair of coefficients depending on the breakwater slope α and γ_f a coefficient accounting for the slope roughness (see OWEN (1980) for values of these coefficients). The representative period T_m corresponds to an average zero-crossing period.

TAW (2002) and EurOtop (2007, 2018) proposed the following formula:

$$q^* \sqrt{\frac{s_m}{\tan \alpha}} = a \exp \left(-b \left[\frac{R_c^*}{\gamma_f} \sqrt{\frac{s_m}{\tan \alpha}} \right]^c \right) \quad (5)$$

with $\tan \alpha / \sqrt{s_m} = \xi$ the surf-similarity or breaker parameter. When waves do not break, i.e. $\xi > 2$ (approximately), equation (5) can be simplified as:

$$q^* = a \exp \left(-b \left[\frac{R_c^*}{\gamma_f} \right]^c \right) \quad (6)$$

In equations (4), (5) and (6), other coefficients can be considered in the same way as γ_f in order to take into account various configurations, such as the presence of a berm, a crown wall and the angle of incidence of waves on the structure. The parameters (a, b, c) vary between equations (4-6) (OWEN, 1980; EurOtop, 2018).

Following the works of VAN GENT (2000) and LORENZO *et al.* (2000), which considered sea states combining swell and wind waves, T_m was chosen as the period $T_{m_{-1,0}} = m_{-1}/m_0$ derived from the moments m_{-1} and m_0 of the wave spectrum. This work has led to an initial consideration of the combination of swell and wind waves in the calculation of wave overtopping rates through the choice of a suitable mean period.

A second adaptation of equation (6) has been proposed by VAN DER WERF & VAN GENT (2018) following a series of experiments involving bimodal sea states. This adaptation consists in modifying the freeboard height in the presence of swell so that $R'_c = R_c - 0.5H_{m_{0,s}}$, with $H_{m_{0,s}}$ the significant height of the swell alone. In the case of a bimodal sea state, the freeboard is thus reduced by half the swell significant wave height. For a given bimodal sea state, the wave overtopping rate calculated using the VAN DER

WERF & VAN GENT (2018) method is higher than that given by formula (6). However, this formula is not suitable for the present study, as freeboard values such as $R_c < 0.5H_{m_{0,s}}$ are used in our tests (see § 3). Recently, ORIMOLOYE *et al.* (2021) proposed a parametrization of the couple (a, b) in equations (5-6) based on the proportion of swell in the total energy of a bimodal sea state. This parameterization was determined using experiments with breakwaters of various slopes. For all breakwater slopes, the trend was for the wave overtopping to increase as the proportion of swell increased. However, a limitation to this parameterization is that it does not include the physical difference between swell and wind waves, that is the difference in peak period of the wave systems. The formulas proposed by VAN DER WERF & VAN GENT (2018) on the one hand, and ORIMOLOYE *et al.* (2021) on the other, are derived from physical models dealing with the submersion of coastal protections in particular configurations. The physical model presented here, which complements that of ORIMOLOYE *et al.* (2021), differs in that it studies the effect of the presence of rock-armored slope on the breakwater and seeks to characterize a bimodal sea state by a representative period rather than by a "swell proportion".

3. Physical model and experimental set-up

3.1 Specifications

The breakwater was designed to best represent the industrial need that prompted this study. To this end, a breakwater slope of 3:2 was selected (see figure 1). The total height of the breakwater, i.e. the distance between the seabed and the breakwater crest level, $(R_c + h)$ in figure 1, is 20 m at prototype scale. The dimensionless freeboards R_c^* are included between 0.4 and 2. The value of 0.4 corresponds to extreme mean water levels. These water levels allow a comparison with the work of VICTOR *et al.* (2012) (included in EurOtop, 2018) considering similar conditions. According to the literature (e.g. EurOtop, 2018), wave overtopping rates are considered independent of swell period given the steep breakwater slope of the present model. Consequently, a single swell period $T_{p,s} = 8.3$ s (at prototype scale) is chosen. The tested sea states, combining different wind-wave periods $T_{p,c}$ as well as different swell and wind-wave heights, are associated with the letters A to H and listed in Table 1. The choice of different peak periods to describe the wind waves stems from the findings of VILLEFER *et al.* (2021) that the wind-wave period can be modified in the presence of swell. One objective is therefore to examine the effect of the wind-wave period on wave overtopping when a background swell is present.

Tableau 1. Wave combinations composing the sea states used during tests associated with significant wave heights, at prototype scale.

Case	Swell		Wind waves	
	$H_{m0,s}$ (m)	$T_{p,s}$ (s)	$H_{m0,ww}$ (m)	$T_{p,ww}$ (s)
A	1.4	8.3	-	-
B	-	-	1.3	5
C	1.2	8.3	1.2	5
D	0.9	8.3	1.1	5
E	0.9	8.3	1.0	1.8
F	0.9	8.3	0.6	3.3
G	0.9	8.3	0.5	2.8
H	0.75	8.3	1.4	5

As coastal protections are commonly covered with a rock armor, another objective is to study the effect of the armored-layer on wave overtopping for a bimodal sea state. Wave overtopping rates obtained with a smooth slope are therefore compared with those obtained with a rocky slope. The rock armor was composed of a double sub-layer, made up of 0.3-1.1 t rock (nominal diameter $D_n = 0.5-0.75$ m) of thickness $2D_n$, covered by a double layer of 1.1-2.6 t surface-layer ($D_n = 0.75-1$ m), again at prototype scale. This armor was designed in accordance with guidelines from The Rock Manual (CIRIA, 2007) to ensure that the relative porosities and permeabilities of the two layers form an armor stable under wave impact. Such a rock armor, through its roughness, porosity and permeability, helps dissipating part of the energy of waves impacting the breakwater. EurOtop (2018) characterizes the surface chosen in the present study by a "roughness" coefficient $\gamma_f = 0.55$, also characterizing porosity and permeability. The value of this coefficient is equivalent to multiplying the dimensionless freeboard height by around 2 (1/0.55 precisely).

3.2 Wave tank

The series of experiments was carried out in the wind-wave tank of the OSU Institut Pythéas in Marseilles (France). Figure 2 introduces the 40 m long and 2.6 m wide wave tank with a sketch. The still water depth h is 0.73 m. This water depth was the main characteristics that determined our choice of a 1:25 scale for the model.

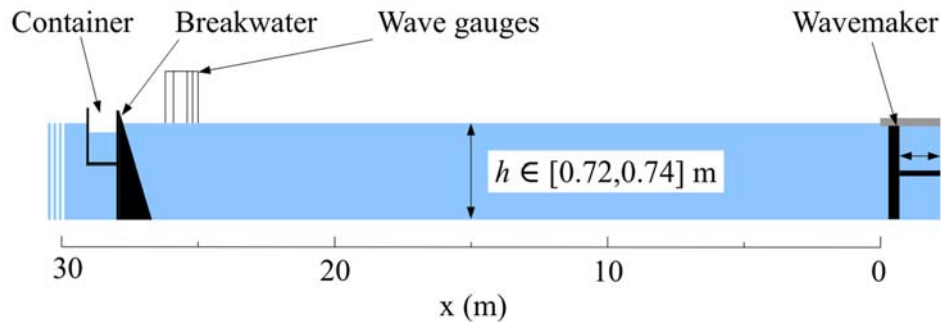


Figure 2. Indicative sketch of the wave tank at OSU Institut Pythéas, showing the position of the breakwater and measuring instruments. The vertical exaggeration is $\times 5$.

The data in Table 1 were used to calculate a JONSWAP-type spectrum (HASSELMANN *et al.* 1973) for each wave system. In the case of bimodal sea states, the JONSWAP spectra for swell and wind waves were added together. From the spectra and considering a set of random phases (uniformly distributed in $[0, 2\pi]$), a temporal free-surface elevation signal was obtained, and then converted into a wavemaker signal (see VILLEFER *et al.* 2021 for details).

3.3 The breakwater models

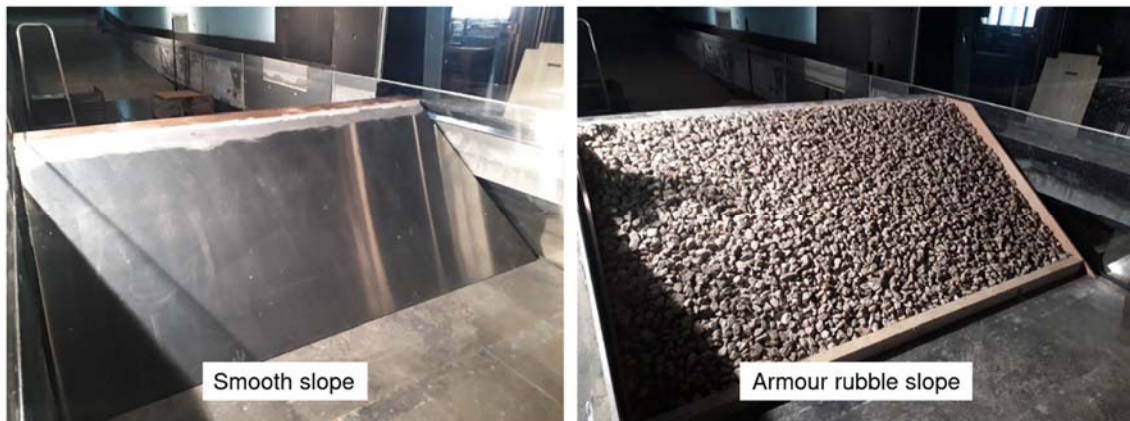


Figure 3. Photographs of the smooth slope breakwater (left) and the armored rubble slope breakwater (right).

The model was installed in the wave flume (see figure 2). One constraint of the flume was that the still water level could only be set between 72 and 74 cm. In order to vary the freeboard height over the selected range of values, it was therefore necessary to be able to vary the breakwater's crest elevation. This was achieved by placing 1.5 cm thick beveled boards on the breakwater crest. The breakwater, initially smooth, was then covered with rocks (see figure 3).

3.4 Measurements

Before each test, a vertical ruler was used to measure the freeboard height R_c . During each test, a sea state from Table 1 was generated for a duration of 30 min, so that at least 1,000 waves impacted the breakwater (in reference to the peak period of the scaled swell). In line with the recommendations of EurOtop (2018), this number of waves impacting the breakwater is necessary in order to obtain data from representative measurement samples. After generation, the waves propagated over about 27 m to the breakwater.

In the case of the smooth breakwater, and to a lesser extent with the rock armor, some of the waves were reflected by the breakwater. In order to separate the incident waves from the reflected ones, a reflection analysis was carried out using a linear least-squares method for unidirectional waves, based on an array of 5 probes positioned relative to the wavelengths of the waves generated (figure 2) (ZELT & SKJELBREIA, 1992).

During each test, the overtopping discharge was collected using a tank connected to a pump, itself connected to a flow meter (see figures 1 and 2) to obtain the wave overtopping rate q averaged over 30 min.

4. Results

Each test carried out with the smooth breakwater or with the rock armor corresponds to a point on figures 4 and 5 respectively. These figures show the nondimensional wave overtopping rate q^* as a function of the dimensional freeboard height R_c^* (see eq. (3)). Each point is colored from blue (dominant swell) to red (dominant wind waves) for increasing values of wave steepness s_m calculated using $T_{m-1,0}$. This choice of representative period follows the results of work by VAN GENT (1999) and LORENZO *et al.* (2000).

4.1 Smooth breakwater

In Figure 4, all test points fall within the confidence interval of formula (6) from EurOtop (2018), defined by $(a, b) = (0.09, 1.5)$ and $\gamma_f = 1$ (smooth breakwater). However, the red dots describe a slightly different slope relative to the blue dots. This results in a slight vertical shift for small values of R_c^* , with the wave overtopping rates due to wind waves slightly lower than those due to swell. Points corresponding to sea states combining swell and wind waves fall between the "pure wind waves" and "pure swell" cases (i.e. red and blue points respectively).

The EurOtop formula proves to be suitable for estimating wave overtopping rates for cases with bimodal sea states and a smooth breakwater with a 3:2 slope. In Figure 4, other choices of pairs (a, b) for equation (6) are given according to the work of VICTOR *et al.* (2012) and ORIMOLOYE *et al.* (2021). The curve of VICTOR *et al.* (2012), designed

for breakwater with steep slopes and low relative freeboard, is suitable for predicting overtopping discharges obtained at low relative freeboard in our case. The formulas of ORIMOLOYE *et al* (2021) show a similar trend to that observed in our case, with higher overtopping rates for pure swell cases (i.e. case A). However, the slope of the red dashed curve, corresponding to the pure wind sea case, does not match that described by the red dots from our tests.

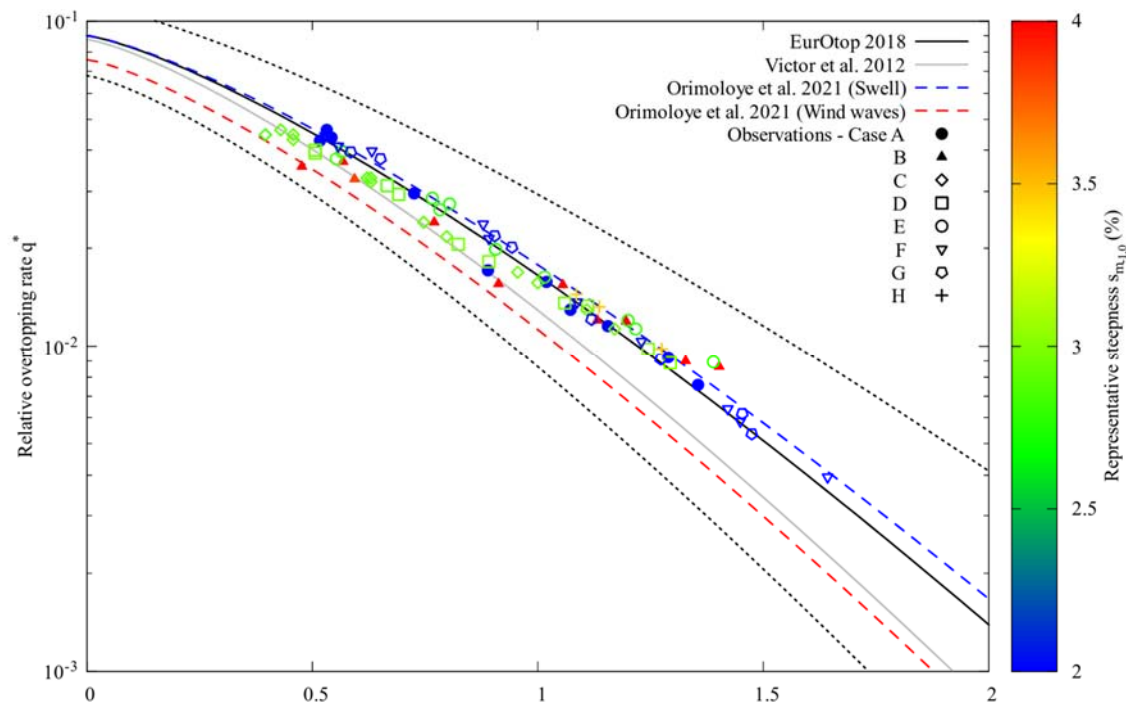


Figure 4. Dimensionless wave overtopping rate as a function of dimensionless freeboard for the smooth breakwater. Each point corresponds to the result of a 30-min test. The points are colored by the representative steepness of the sea state. The dotted black line is the 90 % confidence interval of EurOtop (2018) formula.

4.2 Rock-armored breakwater

In Figure 5, formula (6) from EurOtop 2018 is defined by the same pair (a, b) as for the smooth breakwater with $\gamma_f = 0.4$ to take into account the presence of the rock armor. Some points fall outside the dotted confidence interval at low R_c^* . As the points outside the confidence interval correspond to sea state cases combining swell and wind waves, it seems that the presence of the rock armor provides more effective damping of short-period waves (i.e. wind waves). The difference in slope between the curves described by the points from cases A and B (i.e. pure wind waves and pure swell) is again observed, and more marked than in the case of the smooth breakwater.

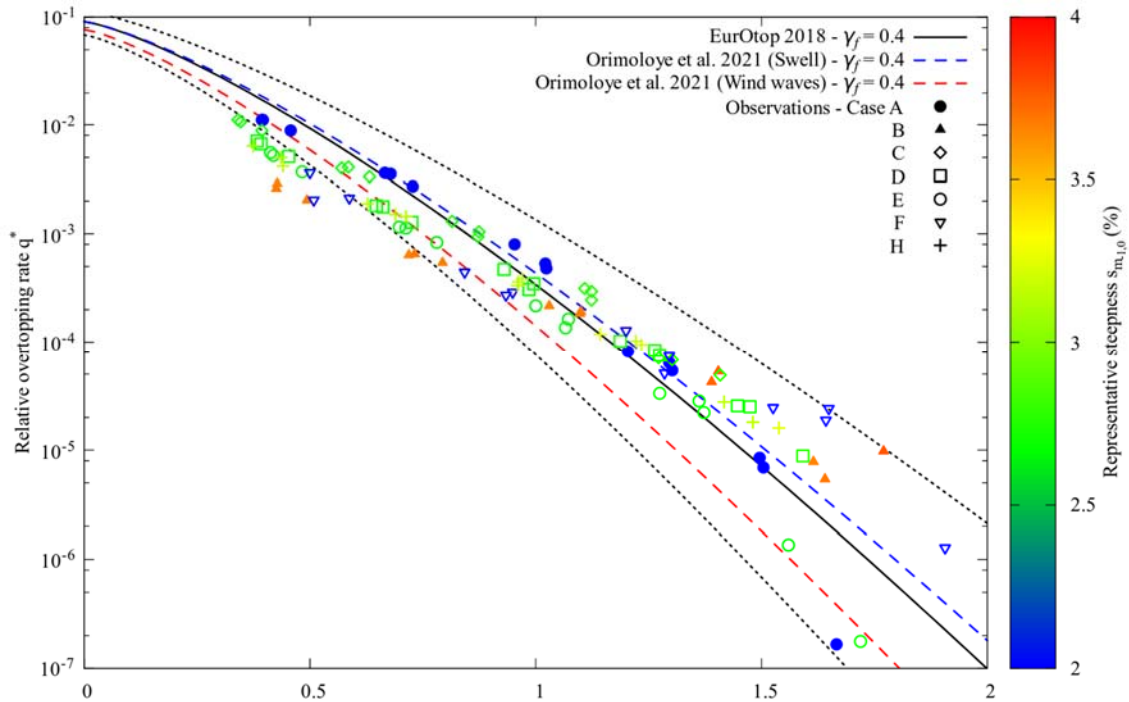


Figure 5. Dimensionless wave overtopping rate as a function of the dimensionless freeboard height for the rock-armored breakwater. Each point corresponds to the result of a 30-min test. The points are colored by the representative steepness of the sea state. A roughness coefficient $\gamma_f = 0.4$ is applied in equation (6) for EurOtop (2018) and ORIMOLOYE *et al.* (2021). The dotted black line is the 90 % confidence interval of EurOtop (2018) formula.

The EurOtop (2018) formula is suitable for the overtopping rates observed in our case for relative freeboard heights greater than around 0.7. On the other hand, for low values of R_c^* , the formula overestimates overtopping rates corresponding to a sea state composed of wind waves alone or swell and wind waves. The red curve given by the ORIMOLOYE *et al.* (2021) formula also overestimates wave overtopping rates for cases with high representative steepness.

5. Discussion

According to Figure 4 for the smooth breakwater, slight differences distinguish the wave overtopping rates relative to the different sea states tested and characterized by a representative steepness. These results, within the confidence interval (at a 90% accuracy level) given in EurOtop (2018), do not question the validity of equation (6). On the other hand, Figure 5 for the rock-armored breakwater shows an amplification of the differences observed previously, leading to a significant overestimation of wave overtopping rates by EurOtop (2018) for sea states with a high representative steepness.

The differences observed between the smooth and rock-armored breakwater cases suggest that the rock armor dissipates the energy of short-wavelength waves (i.e. wind waves)

more efficiently. The wavelength of incident waves, which is not taken into account in equation (6) for a 3:2 slope breakwater (cf. EurOtop, 2018), seems to play an important role in this case.

A first possibility for modifying equation (6) would therefore be to take the representative steepness into account, as in the case of a gentle-slope breakwater (see equation (5)), in the calculation of nondimensional overtopping rates and freeboards. Finally, since wave damping by the various rock layers depends on the type, size and arrangement of the rocks used, we could imagine a second modification based on the definition of a dimensionless number depending on the wavelength and the characteristics of the rock armor.

5. Conclusion

When a sea state is composed of swell and wind waves, EurOtop's (2018) formulas seem suitable for estimating wave overtopping rates on a smooth breakwater. On the other hand, when the breakwater slope has a rock armor, these formulas tend to overestimate the wave overtopping rate. Based on the different cases studied here, this overestimation of overtopping rates was associated with a high representative steepness of the sea state. In the present study, high representative wave steepness corresponds to waves with short wavelengths (i.e. wind waves).

However, the number of configurations experimentally tested remains limited. In order to better characterize the overtopping phenomenon for a bimodal sea state, it would at least be necessary to consider the effect of different types of armored layers and different breakwater slope angles.

6. References

- CIRIA, (2007). *The Rock Manual: The Use of Rock in Hydraulic Engineering*, 2nd ed. C683, CIRIA, London.
- HASSELMANN K., BARNETT T., BOUWS E., CARLSON H., CARTWRIGHT D., ENKE K., EWING J.A., GIENAPP H., HASSELMANN D.E., KRUSEMAN P., MEERBURG A., MULLER P., OLBERS D.J, RICHTER K., SELL W., WALDEN H. (1973). *Measurements of wind-wave growth and swell decay during the Joint North Sea Wave Project (JONSWAP)*. Deutsches Hydrographisches Institut, Vol. 8, pp 1–95.
- LORENZO A., VAN DER MEER J.W., HAWKES P. (2000). *Effects of bi-modal waves on overtopping: Application of UK and Dutch prediction methods*. ASCE, Proc. 27th International Conference on Coastal Engineering, Sydney, Australia, Vol. 3, pp 2114-2127.
- ORIMOLOYE S., HERRILLO-CARABALLO J., KARUNARATHNA H., REEVE D.E. (2021). *Wave overtopping of smooth impermeable seawalls under unidirectional bimodal sea conditions*. Coastal Engineering, Vol. 165, pp 103792. <https://doi.org/10.1016/j.coastaleng.2020.103792>

- OWEN M. (1980). *Design of seawalls allowing for wave overtopping*. Technical report EX924, HR Wallingford, UK.
- PULLEN T., ALLSOP N.W.H., BRUCE T., KORTENHAUS A., SCHÜTTRUMPF H., VAN DER MEER J.W. (2007). *Eurotop Wave Overtopping of Sea Defences and Related Structures: Assessment Manual*. Boyens Medien GmbH. 178 p.
- TAW. (2002). *Wave run-up and wave overtopping at dikes*. Technical report, Technical Advisory Committee on Flood Defence, Delft, The Netherlands.
- VAN DER MEER J.W., ALLSOP N.W.H., BRUCE T., DE ROUCK J., KORTENHAUS A., PULLEN T., SCHÜTTRUMPF H., TROCH P., ZANUTTIGH B. (2018). *Manual on wave overtopping of sea defences and related structures. An overtopping manual largely based on European research, but for worldwide application*. EurOtop Manual. 264 p.
- VAN DER WERF I., VAN GENT, M.R.A. (2018). *Wave overtopping over coastal structures with oblique wind and swell waves*. Journal of Marine Science and Engineering. Vol. 6(4), pp 149. <https://doi.org/10.3390/jmse6040149>
- VAN GENT M.R.A. (1999). *Wave run-up and wave overtopping for double-peaked wave energy spectra*. Delft Hydraulics Report H3351, January 1999, Delft, The Netherlands.
- VAN GENT M.R.A. (2000). *Wave run-up on dikes with shallow foreshores*. ASCE, Proc. 27th International Conference on Coastal Engineering, Sydney, Australia, Vol. 3, pp 2030-2043.
- VICTOR L., VAN DER MEER J.W., TROCH P. (2012). *Probability distribution of individual wave overtopping volumes for smooth impermeable steep slopes with low crest freeboards*. Coastal Engineering. Vol. 64, pp 87–101. <https://doi.org/10.1016/j.coastaleng.2012.01.003>
- VILLEFER A., BENOIT M., VIOLEAU D., LUNEAU C., BRANGER H. (2021). *Influence of Following, Regular, and Irregular Long Waves on Wind-Wave Growth with Fetch: An Experimental Study*. Journal of Physical Oceanography, Vol. 51, pp 3435-3448. <https://doi.org/10.1175/JPO-D-21-0050.1>
- ZELT J.A., SKJELBREIA J.E. (1992). *Estimating incident and reflected wave fields using an arbitrary number of wave gauges*. ASCE, Proc. 23rd International Conference on Coastal Engineering, Venice, Italy, pp. 777-788.